Spectral calibration of exponential Lévy Models [2]

Denis Belomestny*
Markus Reiß**

* Weierstrass Institute for Applied Analysis and Stochastics, Berlin, Germany
** Institute of Applied Mathematics, Ruprecht-Karls-Universität Heidelberg, Germany

BERLIN

ECONOMIC RISK

SFB 649

SPECTRAL CALIBRATION OF EXPONENTIAL LEVY MODELS

DENIS BELOMESTNY AND MARKUS REISS

1. INTRODUCTION

The calibration of financial models has become rather important topic in recent years mainly because of the need to price increasingly complex options in a consistent way. The choice of the underlying model is crucial for the good performance of any calibration procedure. Recent empirical evidences suggest that more complex models taking into account such phenomenons as jumps in the stock prices, smiles in implied volatilities and so on should be considered. Among most popular such models are Levy ones which are on the one hand able to produce complex behavior of the stock time series including jumps, heavy tails and on other hand remain tractable with respect to option pricing. The work on calibration methods for financial models based on Lévy processes has mainly focused on certain parametrisations of the underlying Lévy process with the notable exception of Cont and Tankov (2004). Since the characteristic triplet of a Lévy process is a priori an infinite-dimensional object, the parametric approach is always exposed to the problem of misspecification, in particular when there is no inherent economic foundation of the parameters and they are only used to generate different shapes of possible jump distributions. In this work we propose and test a non-parametric calibration algorithm which is based on the inversion of the explicit pricing formula via Fourier transforms and a regularisation in the spectral domain.Using the Fast Fourier Transformation, the procedure is fast, easy to implement and yields good results in simulations in view of the severe ill-posedness of the underlying inverse problem.

2. Description of the method

Let the prices $Y_1, \ldots, Y_N$ of N call options at strikes $K_1 < \ldots < K_N$ be observable

2.1. **Data transformation.**
We transform the observations (K_j, Y_j) to (x_j, O_j) by

$$O_j := Y_j/S - (1 - K_j e^{-rT}/S)^+,$$
$$x_j := \log(K_j/S) - rT,$$

where T is the time to maturity, r is a short rate and S is the spot price.

2.2. **Estimation of $\mathcal{O}$.**
Find function $\tilde{O}$ among all functions O with two continuous derivatives that minimizes the penalized residual sum of squares

$$(1) \quad \text{RSS}(O, \varkappa) = \sum_{i=0}^{N+1} (O_i - O(x_i))^2 + \varkappa \int_{x_0}^{x_{N+1}} [O''(u)]^2 \, du,$$

where $x_0 \ll x_1$ and $x_{N+1} \gg x_N$ are two artificial points and $O_{N+1} = O_0 = 0$. The first term in (1) measures closeness to the data, while the second term penalizes curvature in the function, and $\varkappa$ establishes a tradeoff between the two. The two special cases are $\varkappa = 0$ when $\tilde{O}$ interpolates the data and $\varkappa = \infty$ when the simple least squares line is fitted. It can be shown that that (1) has an explicit, finite dimensional, unique minimizer which is a natural cubic spline with knots at the unique values of x_i, $i = 1, \ldots, N$. The general cross validation can be used to choose $\varkappa$ (see, for example, Green and Silverman (1994)). Note, that due to the non-smooth behavior of $\mathcal{O}(x)$ at 0 (see Belomestny and Reiß (2004)) it is more reasonable to fit smoothing splines separately for $x > 0$ and $x \leq 0$ and combine them thereafter.

2.3. **Estimation of $\mathcal{FO}$.**
Since the solution of (1) is a natural cubic spline, we can write

$$\tilde{O}(x) = \sum_{j=1}^{N} \theta_j \beta_j(x)$$

where $\beta_j(x)$, $j = 1, \ldots, N$ are set of basis function for representing the family of natural cubic splines. Now we estimate $\mathcal{FO}(v + i)$ by

$$\mathcal{F}\tilde{O}(v + i) = \sum_{j=1}^{N} \theta_j \mathcal{F}[e^{-x}\beta_j(x)](v).$$

Although $\mathcal{F}[e^{-x}\beta_j(x)]$ can be computed in the closed form we prefer using FFT and compute $\mathcal{F}\tilde{O}(v+i)$ on the grid.

2.4. Estimation of ψ. Calculate

$$(2) \qquad \tilde{\psi}(v) := \frac{1}{T}\log\Big(1 + v(v+i)\mathcal{F}\tilde{O}(v+i)\Big), \quad v \in \mathbb{R},$$

where $\log(\cdot)$ is taken in such a way that $\tilde{\psi}(v)$ is continuous with $\tilde{\psi}(-i) = 0$.

2.5. Estimation of σ, γ and λ. With an estimate $\tilde{\psi}$ of ψ at hand, we obtain estimators for the parametric part $(\sigma^2, \gamma, \lambda)$ by an averaging procedure taking into account the polynomial structure of ψ. Upon fixing the spectral cut-off value U, we set

$$(3) \qquad \hat{\sigma}^2 := \int_{-U}^{U} \mathrm{Re}(\tilde{\psi}(u))w_\sigma^U(u)\,du,$$

$$(4) \qquad \hat{\gamma} := \int_{-U}^{U} \mathrm{Im}(\tilde{\psi}(u))w_\gamma^U(u)\,du,$$

$$(5) \qquad \hat{\lambda} := \int_{-U}^{U} \mathrm{Re}(\tilde{\psi}(u))w_\lambda^U(u)\,du,$$

where the weight functions w_σ^U, w_γ^U and w_λ^U are given explicitly by

$$w_\sigma^U(u) = \frac{r+3}{1-2^{-2/(r+1)}}U^{-(r+3)}|u|^r(1-2\cdot\mathbf{1}_{\{|u|>2^{-1/(r+1)}U\}}), \quad u \in [-U,U],$$

$$w_\gamma^U(u) := \frac{r+2}{2U^{r+2}}|u|^r\,\mathrm{sgn}(u), \quad u \in [-U,U],$$

$$w_\lambda(u) := \frac{r+1}{2(2^{2/(r+3)}-1)}U^{-(r+1)}|u|^r(1-2\cdot\mathbf{1}_{\{|u|<2^{-1/(r+3)}U\}}), \quad u \in [-U,U],$$

and $r > 0$ is a parameter reflecting our priori knowledge about the smoothness of ν.

2.6. Estimation of ν. Define

$$(6) \quad \hat{\nu}(u) := \mathcal{F}^{-1}\Big[\Big(\tilde{\psi}(\cdot) + \frac{\hat{\sigma}^2}{2}x^2 - i\hat{\gamma}x + \hat{\lambda}\Big)\mathbf{K}(x)\Big](u), \quad u \in \mathbb{R},$$

where $\mathbf{K}(x)$ is a compactly supported kernel. In all simulations we take

$$\mathbf{K}(x) = \big(1 - (x/U_\nu)^2\big)^+, \quad x \in \mathbb{R}$$

for some U_ν which may differ from U. The use of an additional cut-off parameter U_ν can improve the quality of $\hat{\nu}$ significantly.

2.7. **Correction of ν.** Due to the estimation error and as a result of the cut-off procedure in (6) the estimate $\hat{\nu}$ can take negative values and needs correcting. Our aim is therefore to find $\hat{\nu}^+$ such that

$$\|\hat{\nu}^+ - \hat{\nu}\|^2_{L^2(\mathbb{R})} \to \min, \quad \inf_{x \in \mathbb{R}} \hat{\nu}^+(x) \geq 0$$

subject to

$$\int_{\mathbb{R}} \hat{\nu}^+(x)\, dx = \int_{\mathbb{R}} \hat{\nu}(x)\, dx.$$

It can be easily shown that the solution of the above problem is given by

$$\hat{\nu}^+(x; \xi) := \max\{0, \hat{\nu}(x) - \xi\}, \quad x \in \mathbb{R}$$

where ξ is chosen to satisfy the equation

$$\int_{\mathbb{R}} \hat{\nu}^+(u; \xi)\, du = \int_{\mathbb{R}} \hat{\nu}(u)\, du.$$

2.8. **Choice of parameters.** In our simulations the following heuristic criteria for choosing the spectral cut-off parameter U^* is employed

$$(7) \qquad U^* = \operatorname{argmin}_U \left| \frac{d}{dU} \hat{\sigma}_U \right|.$$

So, U^* corresponds to the flattest region of the curve $U \to \hat{\sigma}_U$ or in other words the region where $\hat{\sigma}_U$ stabilizes. Other possible approaches to choose U include stagewise aggregation discussed in Belomesnty and Reiß (2005) and risk hull minimization developed by Cavalier and Golubev (2005). As to U^*_ν, it can be found as a point where $\hat{\nu}_U$ stabilizes

$$(8) \qquad U^*_\nu = \operatorname{argmin}_{U_\nu} \left\| \frac{d}{dU_\nu} \hat{\nu}_{U_\nu} \right\|_{L_2}.$$

In the case of real data examples when the Levy model serves as an approximation only the following criteria can be useful. One defines U^* as a solution of the following minimization problem

$$(9) \qquad \inf_U \left[\sum_{i=1}^N |C(K_i; \mathcal{T}_U) - Y_i|^2 + \alpha \int_{\mathbb{R}} |\hat{\nu}''_U(x)|^2\, dx \right], \quad \alpha > 0$$

where $C(K; \mathcal{T}_U)$ is the price at strike K computed using the Levy model with the triplet $\mathcal{T}_U = (\hat{\sigma}_U, \hat{\gamma}_U, \hat{\nu}_U)$.

3. Simulated and Real Data Examples

In this section we present simulated as well as real data examples demonstrating the performance of the calibration algorithm proposed. In our simulations different data designs, sample sizes and noise levels are used in order to investigate the behavior of the procedure in circumstances mimicking real ones. The data design $\{x_i\}$ is chosen to be normally distributed with zero mean and variance $1/3$ and hence is similar to the one observed on the market where much more contracts are settled at the money than in- or out of money. Upon simulating the design, $\{O(x_i)\}$ are computed from the underlying model and then contaminated by the noise with zero mean and variances of the order $\{[\delta O(x_i)]^2\}$.

In section 3.1 the *Merton* jump diffusion model is considered where jumps are normally distributed with mean η and variance v^2

$$\nu(x) = \frac{\lambda}{v\sqrt{2\pi}} \exp\left(-\frac{(x-\eta)^2}{2v^2}\right), \quad x \in \mathbb{R}.$$

The parameter γ in the Lévy triple (σ^2, γ, ν) is uniquely determined by the martingale condition

$$\gamma = -(\sigma^2/2 + \lambda(\exp(v^2/2 + \eta) - 1)).$$

Our choice of parameters

$$\sigma = 0.1, \quad \lambda = 5, \quad \eta = -0.1, \quad v = 0.2$$

implies $\gamma = 0.371$. Note, that under such a choice the mean jump size is negative and the model reflects the important feature observed on the market.

More interesting example of *Kou model* is considered in section 3.2 where Lévy density ν is given by

$$\nu(x) = \lambda\Big(p\lambda_+ e^{-\lambda_+ x}\mathbf{1}_{[0,\infty)}(x) + (1-p)\lambda_- e^{\lambda_- x}\mathbf{1}_{(-\infty,0)}(x)\Big), \quad x \in \mathbb{R}.$$

and λ_+, $\lambda_- \geq 0$, $p \in [0,1]$ are parameters. Again the parameter γ is given explicitly by

$$\gamma = -(\sigma^2/2 + \lambda(p/(\lambda_+ - 1) - (1-p)/(\lambda_- + 1)))$$

and under the choice

$$\sigma = 0.1, \quad \lambda = 5, \quad \lambda_- = 4, \quad \lambda_+ = 8, \quad p = 1/3$$

one has $\gamma = 0.424$. The Kou model allows us to model different tails behavior for positive and negative jumps and hence makes the modelling more realistic.

Finally, in section 3.3 two real data examples are presented. Both data

sets consist of DAX options (put and call) for different maturities and strikes. Lévy models are calibrated separately for each maturity.

3.1. **Merton Model.**

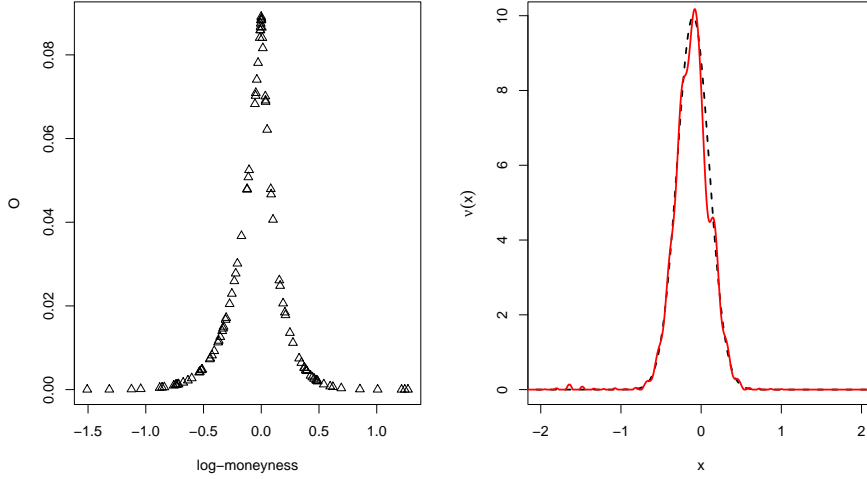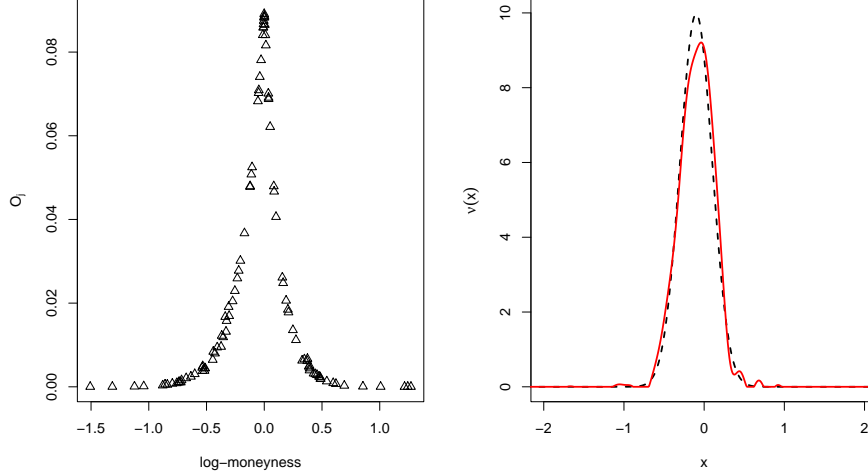Sample Size: $N = 100$

Noise Level: $\delta = 0.05$

FIGURE 1. Left: Sample (O_j). Right: True ν (dashed) and estimated $\hat{\nu}$ (solid) Lévy densities.

$\hat{\sigma}$	$\hat{\gamma}$	$\hat{\lambda}$
0.10402	0.38998	4.90736

TABLE 1. Parameters estimates for the sample shown in Fig. 1 obtained using U and U_ν given by (7) and (8).

$\left[\mathbb{E}(\hat{\sigma}-\sigma)^2\right]^{1/2}$	$\left[\mathbb{E}(\hat{\gamma}-\gamma)^2\right]^{1/2}$	$\left[\mathbb{E}(\hat{\lambda}-\lambda)^2\right]^{1/2}$	$\left[\mathbb{E}\|\hat{\nu}-\nu\|_{L^2}^2\right]^{1/2}$
0.000350	0.003237	0.038097	0.487033

TABLE 2. MSE estimated using 500 Monte Carlo simulations under optimal (oracle) choices of U and U_ν.

Sample Size: $N = 100$
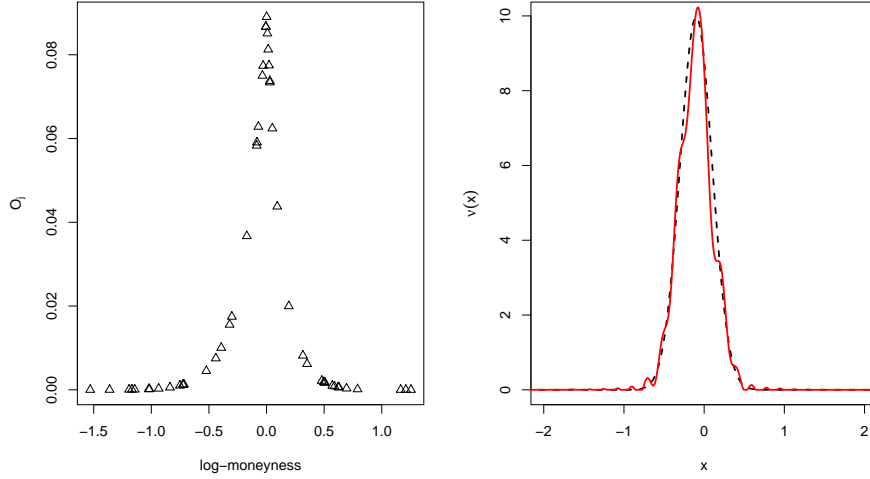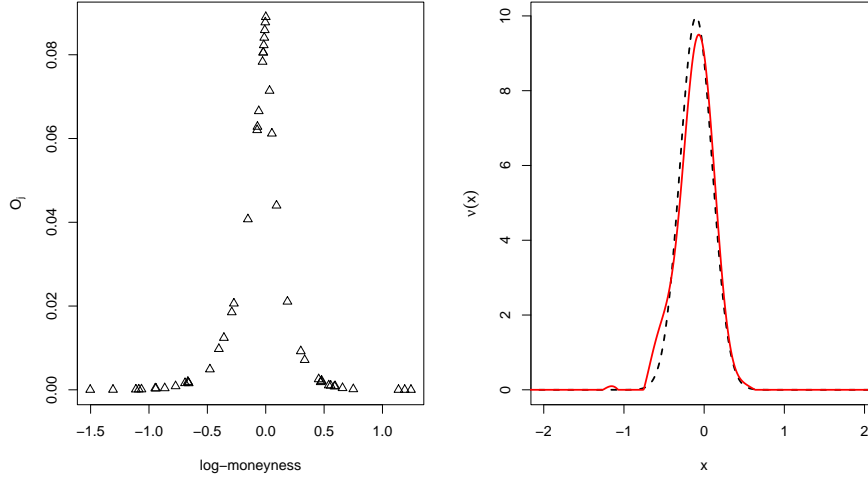
Noise Level: $\delta = 0.1$

FIGURE 2. Left: Sample (O_j). Right: True ν (dashed) and estimated $\hat{\nu}$ (solid) Lévy densities.

$\hat{\sigma}$	$\hat{\gamma}$	$\hat{\lambda}$
0.10208	0.35187	5.06226

TABLE 3. Parameters estimates for the sample shown in Fig. 2 obtained using U and U_ν given by (7) and (8).

$\left[\mathbb{E}(\hat{\sigma} - \sigma)^2\right]^{1/2}$	$\left[\mathbb{E}(\hat{\gamma} - \gamma)^2\right]^{1/2}$	$\left[\mathbb{E}(\hat{\lambda} - \lambda)^2\right]^{1/2}$	$\left[\mathbb{E}\,\|\hat{\nu} - \nu\|_{L^2}^2\right]^{1/2}$
0.000721	0.008502	0.047850	0.632208

TABLE 4. MSE estimated using 500 Monte Carlo simulations under optimal (oracle) choices of U and U_ν.

Sample Size: $N = 50$

Noise Level: $\delta = 0.05$

FIGURE 3. Left: Sample (O_j). Right: True ν (dashed) and estimated $\hat{\nu}$ (solid) Lévy densities.

$\hat{\sigma}$	$\hat{\gamma}$	$\hat{\lambda}$
0.11637	0.38541	4.73875

TABLE 5. Parameters estimates for the sample shown in Fig. 3 obtained using U and U_ν given by (7) and (8).

$\left[\mathbb{E}(\hat{\sigma} - \sigma)^2\right]^{1/2}$	$\left[\mathbb{E}(\hat{\gamma} - \gamma)^2\right]^{1/2}$	$\left[\mathbb{E}(\hat{\lambda} - \lambda)^2\right]^{1/2}$	$\left[\mathbb{E}\left\|\hat{\nu} - \nu\right\|_{L^2}^2\right]^{1/2}$
0.000882	0.013349	0.043730	0.662298

TABLE 6. MSE estimated using 500 Monte Carlo simulations under optimal (oracle) choices of U and U_ν.

Sample Size: $N = 50$

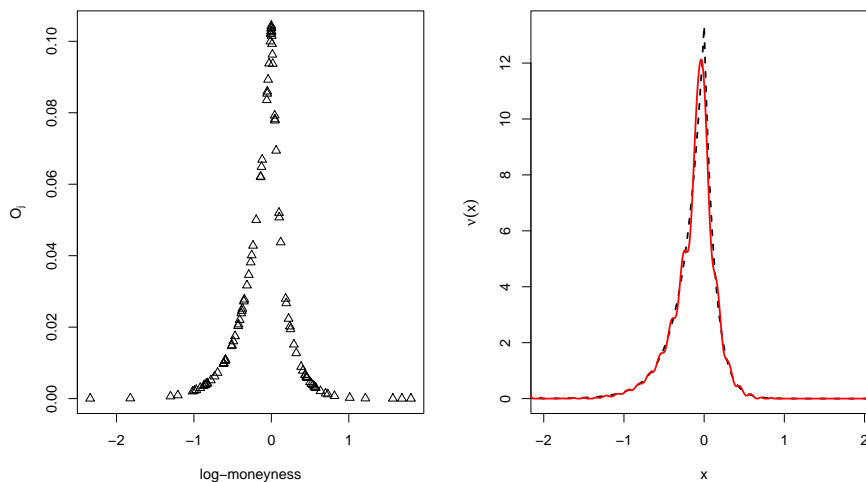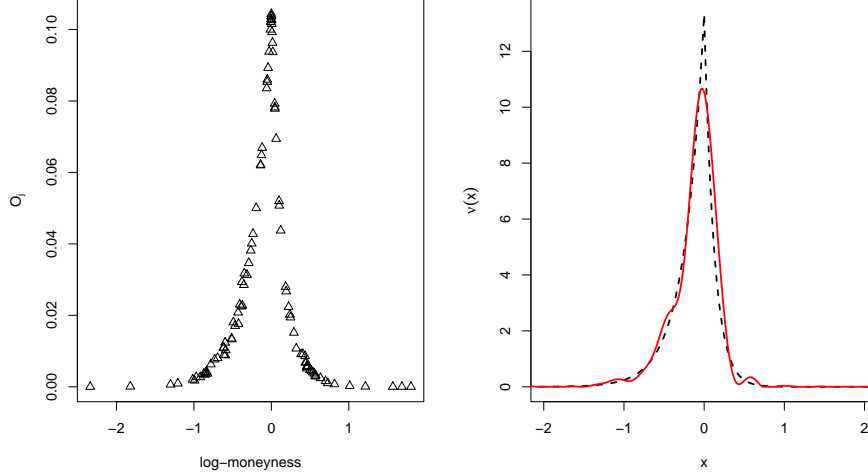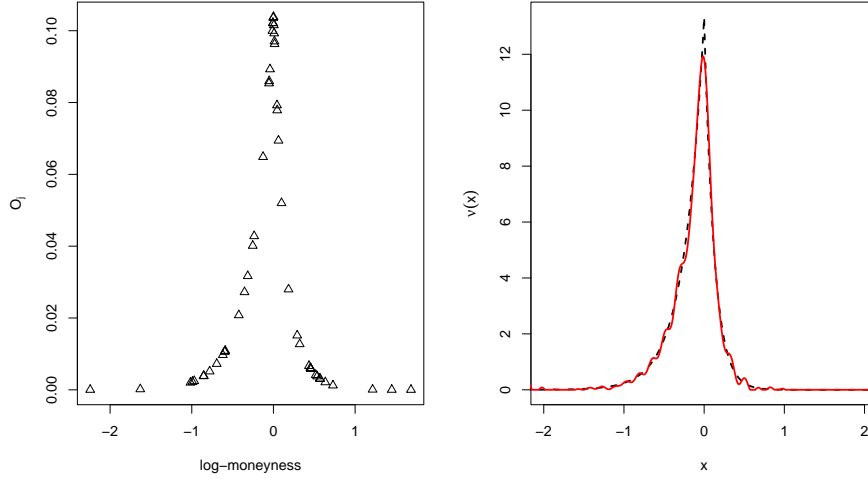Noise Level: $\delta = 0.1$

FIGURE 4. Left: Sample (O_j). Right: True ν (dashed) and estimated $\hat{\nu}$ (solid) Lévy densities.

$\hat{\sigma}$	$\hat{\gamma}$	$\hat{\lambda}$
0.12870	0.36274	4.96426

TABLE 7. Parameters estimates for the sample shown in Fig. 4 obtained using U and U_ν given by (7) and (8).

$\left[\mathbb{E}(\hat{\sigma} - \sigma)^2\right]^{1/2}$	$\left[\mathbb{E}(\hat{\gamma} - \gamma)^2\right]^{1/2}$	$\left[\mathbb{E}(\hat{\lambda} - \lambda)^2\right]^{1/2}$	$\left[\mathbb{E} \|\hat{\nu} - \nu\|_{L^2}^2\right]^{1/2}$
0.001852	0.030394	0.060641	0.859707

TABLE 8. MSE estimated using 500 Monte Carlo simulations under optimal (oracle) choices of U and U_ν.

3.2. **Kou Model.**

Sample Size: $N = 100$

Noise Level: $\delta = 0.05$

FIGURE 5. Left: Sample (O_j). Right: True ν (dashed) and estimated $\hat{\nu}$ (solid) Lévy densities.

$\hat{\sigma}$	$\hat{\gamma}$	$\hat{\lambda}$
0.10071	0.43404	5.04483

TABLE 9. Parameters estimates for the sample shown in Fig. 5 obtained using U and U_ν given by (7) and (8).

$\left[\mathbb{E}(\hat{\sigma} - \sigma)^2\right]^{1/2}$	$\left[\mathbb{E}(\hat{\gamma} - \gamma)^2\right]^{1/2}$	$\left[\mathbb{E}(\hat{\lambda} - \lambda)^2\right]^{1/2}$	$\left[\mathbb{E}\,\|\hat{\nu} - \nu\|_{L^2}^2\right]^{1/2}$
0.001006	0.005631	0.044007	0.662266

TABLE 10. MSE estimated using 500 Monte Carlo simulations under optimal (oracle) choices of U and U_ν.
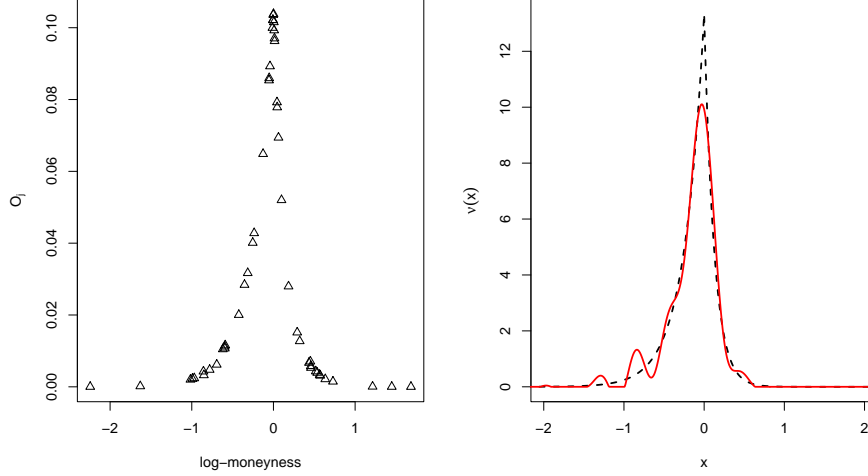
Sample Size: $N = 100$

Noise Level: $\delta = 0.1$

FIGURE 6. Left: Sample (O_j). Right: True ν (dashed) and estimated $\hat{\nu}$ (solid) Lévy densities.

$\hat{\sigma}$	$\hat{\gamma}$	$\hat{\lambda}$
0.09696	0.38269	5.19702

TABLE 11. Parameters estimates for the sample shown in Fig. 6 obtained using U and U_ν given by (7) and (8).

$\left[\mathbb{E}(\hat{\sigma} - \sigma)^2\right]^{1/2}$	$\left[\mathbb{E}(\hat{\gamma} - \gamma)^2\right]^{1/2}$	$\left[\mathbb{E}(\hat{\lambda} - \lambda)^2\right]^{1/2}$	$\left[\mathbb{E}\|\hat{\nu} - \nu\|_{L^2}^2\right]^{1/2}$
0.001786	0.012310	0.054588	0.944580

TABLE 12. MSE estimated using 500 Monte Carlo simulations under optimal (oracle) choices of U and U_ν.

Sample Size: $N = 50$

Noise Level: $\delta = 0.05$

FIGURE 7. Left: Sample (O_j). Right: True ν (dashed) and estimated $\hat{\nu}$ (solid) Lévy densities.

$\hat{\sigma}$	$\hat{\gamma}$	$\hat{\lambda}$
0.10889	0.41842	4.99187

TABLE 13. Parameters estimates for the sample shown in Fig. 7 obtained using U and U_ν given by (7) and (8).

$\left[\mathbb{E}(\hat{\sigma} - \sigma)^2\right]^{1/2}$	$\left[\mathbb{E}(\hat{\gamma} - \gamma)^2\right]^{1/2}$	$\left[\mathbb{E}(\hat{\lambda} - \lambda)^2\right]^{1/2}$	$\left[\mathbb{E}\|\hat{\nu} - \nu\|_{L^2}^2\right]^{1/2}$
0.002444	0.018898	0.064104	0.998157

TABLE 14. MSE estimated using 500 Monte Carlo simulations under optimal (oracle) choices of U and U_ν.

Sample Size: $N = 50$

Noise Level: $\delta = 0.1$

FIGURE 8. Left: Sample (O_j). Right: True ν (dashed) and estimated $\hat{\nu}$ (solid) Lévy densities.

$\hat{\sigma}$	$\hat{\gamma}$	$\hat{\lambda}$
0.13086	0.42390	4.98324

TABLE 15. Parameters estimates for the sample shown in Fig. 8 obtained using U and U_ν given by (7) and (8).

$\left[\mathbb{E}(\hat{\sigma} - \sigma)^2\right]^{1/2}$	$\left[\mathbb{E}(\hat{\gamma} - \gamma)^2\right]^{1/2}$	$\left[\mathbb{E}(\hat{\lambda} - \lambda)^2\right]^{1/2}$	$\left[\mathbb{E}\,\|\hat{\nu} - \nu\|_{L^2}^2\right]^{1/2}$
0.004917	0.037315	0.108304	1.40540

TABLE 16. MSE estimated using 500 Monte Carlo simulations under optimal (oracle) choices of U and U_ν

3.3. **Real Data Examples.**

DAX options, 22 March 1999
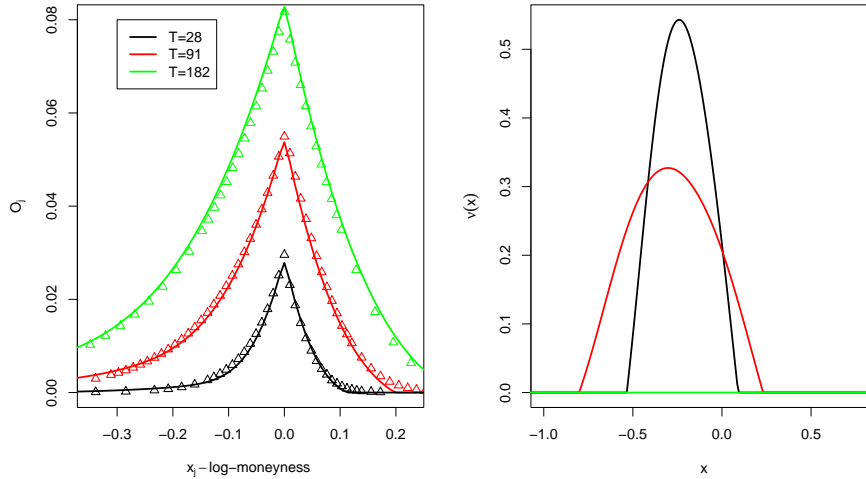
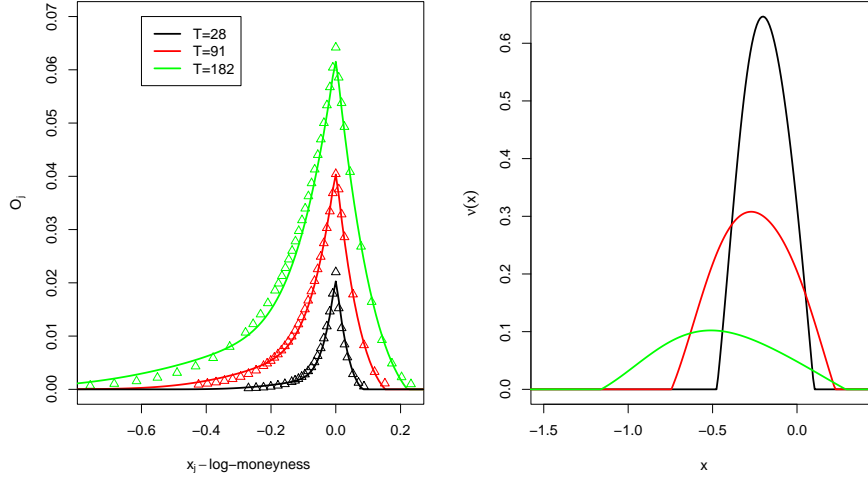
FIGURE 9. Left: Observed (triangles) and fitted (solid line) put ($x_j < 0$) and call ($x_j \geq 0$) prices for different maturities. Right: Estimated Lévy densities.

T	N	$\hat{\sigma}$	$\hat{\gamma}$	$\hat{\lambda}$
28	37	0.0673	0.0379	0.2105
91	56	0.0699	0.0360	0.2118
182	38	0.0819	0.0417	0.0019

TABLE 17. Parameters of Lévy triple estimated from DAX data shown in Fig. 9 with U chosen via the criteria (9) with $\alpha = 1e - 8$

All options data used here are publicly available in MDBase at
http://www.quantlet.org/mdbase

DAX options, 21 Juni 1999

FIGURE 10. Left: Observed (triangles) and fitted (solid line) put ($x_j < 0$) and call ($x_j \geq 0$) prices for different maturities. Right: Estimated Lévy densities.

T	N	$\hat{\sigma}$	$\hat{\gamma}$	$\hat{\lambda}$
28	28	0.0353	0.0416	0.2317
91	38	0.0381	0.0347	0.1876
182	42	0.0446	0.0214	0.0887

TABLE 18. Parameters of Lévy triple estimated from DAX data shown in Fig. 10 with U chosen via the criteria (9) with $\alpha = 1e - 8$

4. Conclusions

- The performance of the procedure depends strongly on the noise level and the number of observations the first being dominating.
- The smoother is the Lévy density the better is the performance of the procedure the difference being more pronounced for smaller noise levels.
- The main features of Lévy measures (different tails behavior, negative mean jump size) are preserved during the reconstruction.
- In the real data examples the algorithm produces stable estimates for σ, λ decreasing with maturity, jump distributions with negative mean jump sizes, and by rather small complexity of Lévy measures fits the data in a reasonable way.

References

[1] Belomestny, D., and M. Reiss (2005) "Optimal calibration of exponential Levy models", Preprint 1017, Weierstraß Institute (WIAS) Berlin.
[2] Cavalier, L. and Y. Golubev (2005) "Risk hull method and regularization by projections of ill-posed inverse problems," *Ann. Stat., to appear.*
[3] Cont, R., and P. Tankov (2004) Nonparametric calibration of jump-diffusion option pricing models, *Journal of Computational Finance*, 7(3), 149.
[4] Green, P. and Silverman, B. (1994). *Nonparametric Regression and Generalized linear Models: A Roughness Penalty Approach*, Chapman and Hall, London.

SFB 649 Discussion Paper Series 2006

For a complete list of Discussion Papers published by the SFB 649, please visit http://sfb649.wiwi.hu-berlin.de.

001 "Calibration Risk for Exotic Options" by Kai Detlefsen and Wolfgang K. Härdle, January 2006.

002 "Calibration Design of Implied Volatility Surfaces" by Kai Detlefsen and Wolfgang K. Härdle, January 2006.

003 "On the Appropriateness of Inappropriate VaR Models" by Wolfgang Härdle, Zdeněk Hlávka and Gerhard Stahl, January 2006.

004 "Regional Labor Markets, Network Externalities and Migration: The Case of German Reunification" by Harald Uhlig, January/February 2006.

005 "British Interest Rate Convergence between the US and Europe: A Recursive Cointegration Analysis" by Enzo Weber, January 2006.

006 "A Combined Approach for Segment-Specific Analysis of Market Basket Data" by Yasemin Boztuğ and Thomas Reutterer, January 2006.

007 "Robust utility maximization in a stochastic factor model" by Daniel Hernández–Hernández and Alexander Schied, January 2006.

008 "Economic Growth of Agglomerations and Geographic Concentration of Industries - Evidence for Germany" by Kurt Geppert, Martin Gornig and Axel Werwatz, January 2006.

009 "Institutions, Bargaining Power and Labor Shares" by Benjamin Bental and Dominique Demougin, January 2006.

010 "Common Functional Principal Components" by Michal Benko, Wolfgang Härdle and Alois Kneip, Jauary 2006.

011 "VAR Modeling for Dynamic Semiparametric Factors of Volatility Strings" by Ralf Brüggemann, Wolfgang Härdle, Julius Mungo and Carsten Trenkler, February 2006.

012 "Bootstrapping Systems Cointegration Tests with a Prior Adjustment for Deterministic Terms" by Carsten Trenkler, February 2006.

013 "Penalties and Optimality in Financial Contracts: Taking Stock" by Michel A. Robe, Eva-Maria Steiger and Pierre-Armand Michel, February 2006.

014 "Core Labour Standards and FDI: Friends or Foes? The Case of Child Labour" by Sebastian Braun, February 2006.

015 "Graphical Data Representation in Bankruptcy Analysis" by Wolfgang Härdle, Rouslan Moro and Dorothea Schäfer, February 2006.

016 "Fiscal Policy Effects in the European Union" by Andreas Thams, February 2006.

017 "Estimation with the Nested Logit Model: Specifications and Software Particularities" by Nadja Silberhorn, Yasemin Boztuğ and Lutz Hildebrandt, March 2006.

018 "The Bologna Process: How student mobility affects multi-cultural skills and educational quality" by Lydia Mechtenberg and Roland Strausz, March 2006.

019 "Cheap Talk in the Classroom" by Lydia Mechtenberg, March 2006.

020 "Time Dependent Relative Risk Aversion" by Enzo Giacomini, Michael Handel and Wolfgang Härdle, March 2006.

021 "Finite Sample Properties of Impulse Response Intervals in SVECMs with Long-Run Identifying Restrictions" by Ralf Brüggemann, March 2006.

022 "Barrier Option Hedging under Constraints: A Viscosity Approach" by Imen Bentahar and Bruno Bouchard, March 2006.